11TH IAG INTERNATIONAL CONFERENCE ON GEOMORPHOLOGY


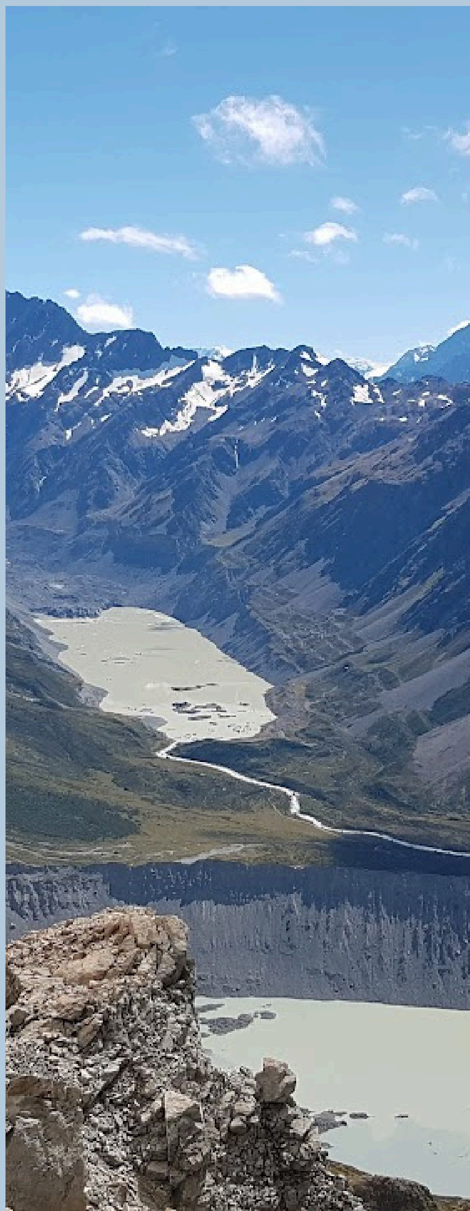


FIELDTRIP GUIDE

EARTHQUAKE FAULTING AND THE LEADER LANDSLIDE DAM

2026

11TH IAG INTERNATIONAL CONFERENCE ON GEOMORPHOLOGY

2–6 February 2026

Christchurch, New Zealand (Ōtautahi, Aotearoa)

COMPILED FOR THE 11TH IAG INTERNATIONAL CONFERENCE ON GEOMORPHOLOGY

ŌTAUTAHI, AOTEAROA
CHRISTCHURCH, NEW ZEALAND
2026

Cover Photos: Wairongomai-Mangarara (Credit: Ian Fuller), Aoraki Mt. Cook National Park (Credit: Sam McColl), and Waikato at Taupo (Credit: Sarah McSweeney).

Earthquake faulting and the Leader Landslide dam

Andy Nicol [1] and Anna McCarthy[1]

Affiliation 1. School of Earth and Environment, University of Canterbury, Christchurch, New Zealand

Introduction

The fieldtrip will take participants to the epicentral area of the 2016 Mw 7.8 Kaikōura Earthquake in North Canterbury (Figure 1). The landscape in this region includes flights of Late Quaternary fluvial terraces, tectonic basins and ranges, and landslides. The formation of these landforms is strongly influenced by active Earth deformation and seismic shaking during large earthquakes. We will examine geomorphology produced by surface rupture and ground shaking during the Kaikōura earthquake. The trip will visit fault scarps and displaced fences produced by surface ruptures, together with a large intact landslide dam (Nicol et al. 2018; McCarthy 2025). Participants will have the opportunity to observe the Leader River as it is re-establishing itself across the large Leader landslide. During the fieldtrip we will see a landscape that has evolved rapidly since the earthquake and discuss the natural hazards posed by earthquake-related processes.

In the following sections we provide background material for the fieldtrip and more detailed descriptions of each stop. This fieldtrip guide will be augmented by discussions during the fieldtrip.

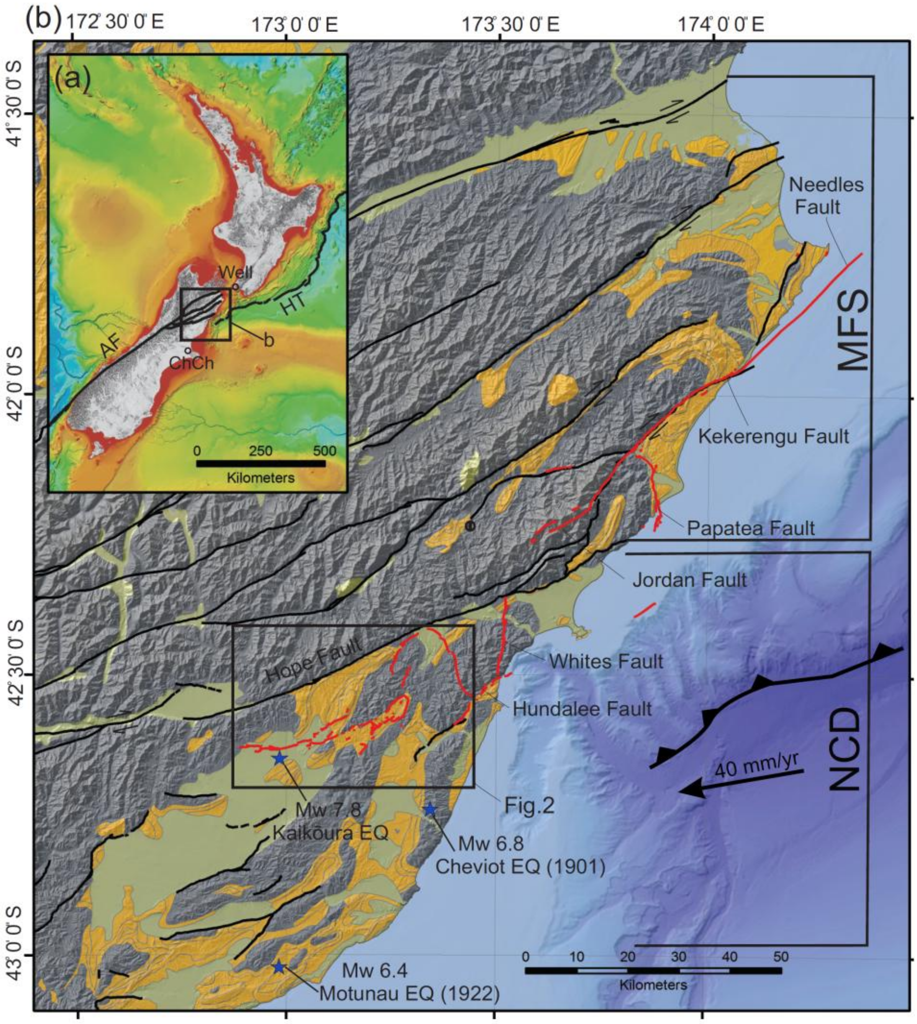

Figure 1. *Maps showing the plate boundary setting of the Kaikōura earthquake. (a) New Zealand plate boundary. AF, Alpine Fault; ChCh, Christchurch; HT, Hikurangi Trough; Well, Wellington. (b) Geology (Torlesse Supergroup Basement - grey; Late Cretaceous-Cenozoic strata – orange-brown; Quaternary deposits – yellow-green; Rattenbury et al., 2006), active faults (black lines from Langridge et al. 2016) and faults that ruptured in the November 14 2016 M_w 7.8 Kaikōura earthquake (red lines with fault names) in the northeastern South Island. The Pacific Plate motion vector relative to the Australian Plate is from Beavan et al. (2002). MFS, Marlborough Fault System; NCD, North Canterbury Domain. Figure from Nicol et al. (2018).*

Kaikōura Earthquake and geological setting

The Mw 7.8 Kaikōura earthquake struck almost 10 years ago at two minutes past midnight on 14 November 2016 (NZDT). Its epicentre was located near the South Island township of Waiau (Figures 1 & 2), where we will be visiting today. The Kaikōura earthquake ruptured at least 20 faults at the ground surface for a distance of ~165 km across the plate boundary zone in the northeastern South Island of New Zealand (Figure 1). The earthquake initiated at a focal depth of ~14 km on The Humps Fault (Figures 1 & 2) and propagated northwards with the greatest energy release occurring north of Kaikōura (Kaiser et al., 2017; Hamling et al., 2017). Although damage to housing, farm infrastructure and the transport network was extensive, only two deaths were attributed to the earthquake. The low number of fatalities reflect the mostly rural setting of the earthquake and its timing; if the earthquake struck in the middle of the day the number of fatalities could have been significantly higher.

The complexity of the Kaikōura earthquake is partly reflected in the oblique focal mechanism, which displays approximately equal components of thrusting/reverse and right-lateral slip (e.g., Cesca et al., 2017; Kaiser et al., 2017; Wang et al., 2017). The resulting fault ruptures displaced the ground surface and sea floor with strikes varying from east-west to north-northwest. The east-northeast striking faults are primarily right-lateral strike-slip and the northerly striking faults have left-lateral reverse displacement (Litchfield et al., 2018; Nicol et al., 2018). In addition to the mapped surface faults, the spatial extent of coastal uplift and widespread occurrence of tsunami up to ~250 km from Kaikōura have been interpreted to indicate slip on the subduction interface and/or a blind upper plate thrust(s) within the accretionary prism complex (e.g., Clark et al., 2017; Wang et al., 2017; Mouslopoulou et al., 2019).

The Kaikōura earthquake produced displacement on faults that accommodate the transition from subduction beneath the North Island to continental collision and strike slip on the Alpine fault in the South Island of New Zealand (Figure 2a). Onshore in the South Island, ~75% of the ~40 mm/yr relative plate motion is transferred from subduction towards the Alpine fault via strike-slip on the Marlborough Fault System (MFS) (e.g., Beavan and Haines, 2001; Wallace et al., 2012). Offshore and east of the Kaikōura earthquake surface ruptures, plate boundary deformation is accommodated by a subduction thrust and accretionary prism complex (e.g., Barnes and Audru, 1999; Williams et al., 2013). The accretionary prism and eastern MFS are underlain by the Pacific plate which, based on seismic tomography and focal depths of historical seismicity, extends to a depth of at least 200 km beneath the northern South Island (e.g., Eberhart-Phillips and Bannister, 2010; Williams et al., 2013). These data indicate that in the epicentral area the top of the subducted Pacific plate is located at a depth of ~20-30 km beneath the surface ruptures and may define the lower limit of the upper-plate faults (Nicol et al., 2018).

In North Canterbury, here referred to as the North Canterbury (Tectonic) Domain (NCD) (Figure 2), active faulting and Quaternary deformation has been widely reported prior to the Kaikōura earthquake (e.g., Pettinga et al., 2001; Rattenbury et al., 2006; Forsyth et al., 2008; Barrell and Townsend, 2012). The NCD accommodates transpression and is dominated by northeast-striking oblique-slip faults with components of right-lateral and reverse displacement (e.g., Nicol et al., 1994; Pettinga et al., 2001). These faults typically separate hanging-wall anticlines and footwall synclines, which are manifest in the topography as Quaternary-age ranges and basins. Late Cretaceous to Pliocene strata, that predate the onset of Quaternary deformation, and Quaternary gravels occupy the basins, while the ranges are typically cored by Mesozoic Torlesse Supergroup basement (Figure 2) and can reach altitudes of ~1000 m (e.g., Warren, 1995; Rattenbury et al., 2006; Forsyth et al., 2008).

River systems in North Canterbury produce terrace surfaces that range in lateral extent and height above their active riverbed. In the basins river terraces are laterally extensive, forming wide alluvial plains, while proximal to the basin margins and across the ranges (where the rivers are deeply incised), the river terraces are of limited size (e.g., Rattenbury et al., 2006). These terraces typically comprise the Last Glacial Maxima (LGM) aggradation surface (abandoned 10-20 kyr ago), incised by flights of degradation terraces. Geomorphic mapping indicates at least 12 degradation terraces below the inferred LGM surface in the Leader River and Leader landslide area (McCarthy 2025). On the Emu Plains, which were displaced by The Humps Fault during the 2016 earthquake, may locally reach ~70 kyr in age (Rattenbury et al., 2006).

Many of the faults mapped in the NCD are associated with active fault traces, which attest to the ongoing earthquake activity of these structures (e.g., Pettinga et al., 2001; Rattenbury et al., 2006; Forsyth et al., 2008; Barrell and Townsend, 2012). Quantitative data constraining the displacement rates and recurrence intervals of these faults is limited, with the majority of rates estimated to be <2 mm/yr and recurrence intervals of thousands to 10s of thousands of years (Pettinga et al., 2001; Barrell and Townsend, 2012; Brough et al., 2023). Due in part to these long recurrence intervals the faults that ruptured in the NCD on November 14 2016 were either, not known to be active or their lengths were poorly defined prior to the earthquake. Given these recurrence intervals it is also unsurprising that the Kaikōura earthquake is the only historical event to have produced surface rupture in the NCD. In addition to the Kaikōura earthquake the M_w 6.8 Cheviot 1901 and M_w 6.4 Motunau 1922 shallow (<25 km depth) earthquakes may have produced surface folding in the NCD due to fault displacement at depth (see Downes and Dowrick, 2015, for descriptions of the earthquakes and Figure 1 for their locations).

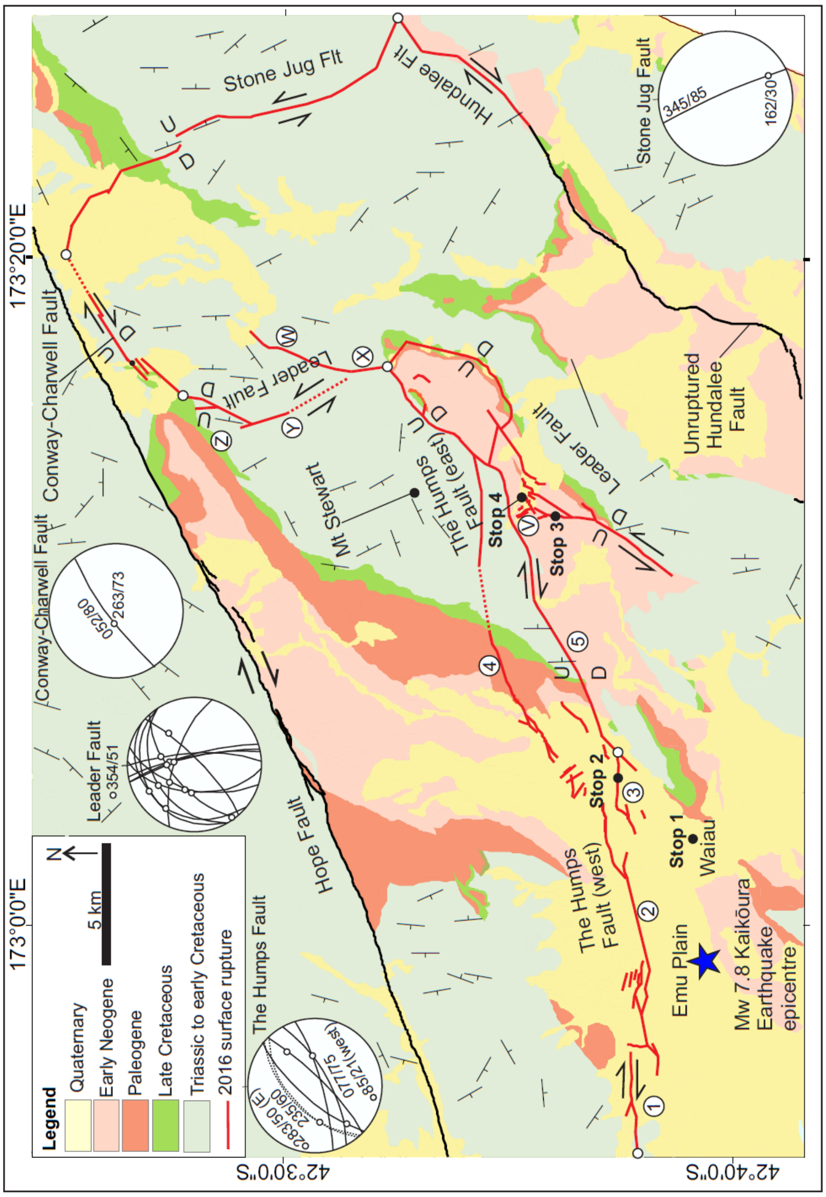

Figure 2. *Geological map of rock units, active faults that did not rupture during the earthquake (dark grey lines) and surface ruptures from the Kaikōura earthquake (solid and black lines surveyed and dashed redlines inferred from deformation recorded by InSAR in the study area south of the Hope fault in the NCD (Rattenbury et al., 2006; Langridge et al., 2016). Strike and dip of bedding in Torlesse rocks is from Rattenbury et al. (2006). See Figure 1 for location of Figure 2. Inset stereonets depict fault planes (great circles) and slip vectors (white filled circles) for The Humps, Leader, Conway-Charwell and Stone Jug faults from field measurements. Strike-slip movement sense shown by arrows along with upthrow (U) and down throw (D) on fault traces. Locations of stops 1, 2, 3 and 4 shown. Figure modified from Nicol et al. (2018).*

Leader landslide and dam

The Kaikōura Earthquake triggered almost 30,000 landslides over an area 10,000 km^2 (e.g., Massey et al. 2018, 2020). In Leader River catchment, ground motions during the Kaikōura Earthquake initiated hundreds of co-seismic landslides, the largest of which was the Leader landslide (Figure 3). The Leader landslide generated a deposit of approximately 600,000m^2 in area (volume 6-8 million m^3), with a head-scarp 400 m wide and 200 m high (Gray, 2018)(Figure 3). The Leader landslide resulted from failure of the southern face of Mount Steward which travelled up to 250 m vertically and was deposited into the deeply incised Leader River valley. Landslide debris buried approximately ~980m of the active riverbed and dammed the river (McCarthy, 2025). In the weeks following the earthquake, Lake Rebekah formed upstream of the landslide dam (Figure 3).

Figure 3. *Aerial view of the Leader landslide (view to the northeast). Note Lake Rebekah immediately upstream of the landslide debris and minor flow along the landslide-debris margin in the foreground. Photograph by Kate Pedley 6/12/17.*

In the nearly ten years since the earthquake, the Leader River has down-cut into landslide debris, fluvial terrace deposits and bedrock (e.g., Figure 4). River erosion was primarily achieved by a combination of upstream knickpoint migration (Figure 4) and dam-overtopping events. Despite river erosion, the landslide dam has not been completely breached, and Lake Rebekah remains today, in part due to landowner intervention in 2017 to stabilize the landslide along the active riverbed.

LiDAR, satellite aerial imagery, drone surveys and landowner communication from 2001 to 2024 were used to chart the evolution of the active riverbed pre- and post-earthquake for up to 2 km downstream of Lake Rebekah (McCarthy 2025). Despite the stability of Lake Rebekah, these data show that the position and morphology of the Leader River has changed significantly to accommodate the landslide, with the formation of two knickpoint waterfalls up to 14m high, three waterbodies (two current, one past), and diversion of the river around the landslide toe (Figures 3 & 4). Evolution of the river is characterised by long periods of stasis (e.g. months to years) punctuated by rapid changes in riverbed morphology (hours to weeks) associated with incision and aggradation. Here we present the history of river evolution and consider factors impacting riverbed morphology. Factors impacting the evolution of river-bed include, rain-storm events, partial lake outburst flooding, spatial changes in Pliocene-Miocene siltstone bed induration and farmer intervention (McCarthy, 2025).

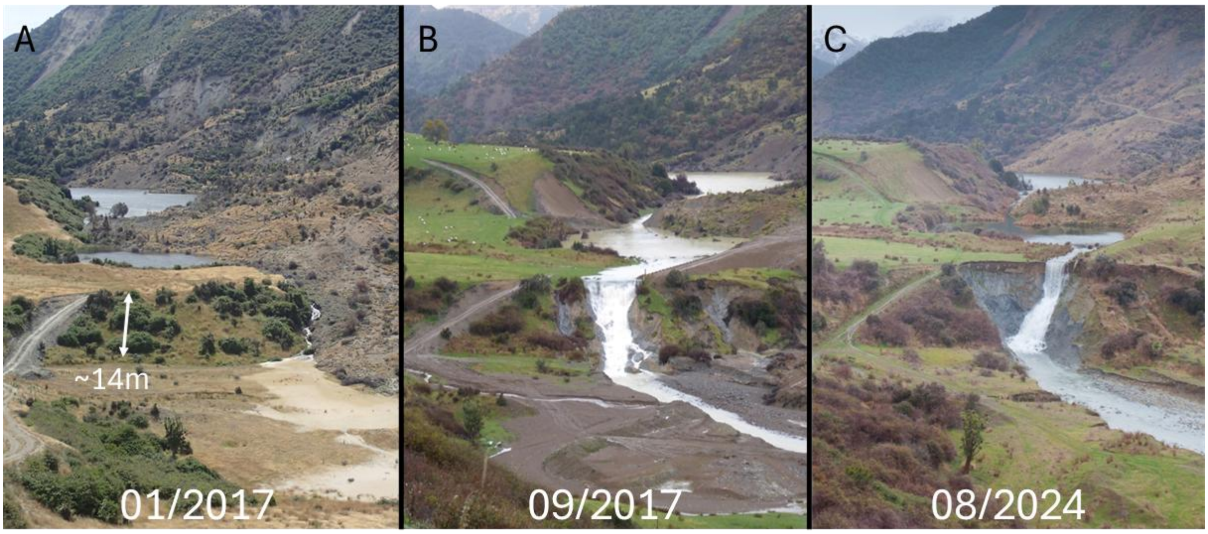

Figure 4. *Photographs of the western knickpoint viewed from the nearby Last Glacial Maxima terrace surface. From left to right, images were taken in January 2017, September 2017 and August 2024. Photos courtesy of Kate Pedley. Figure from McCarthy (2025).*

Implications for hazards

The Kaikōura earthquake and Leader landslide have implications for the identification and characterisation of hazards. Prior to the Kaikōura earthquake knowledge of the locations, geometries and paleoearthquake histories of the faults that ruptured was incomplete. North of the Hope Fault within the MFS, most of the main faults (e.g., >1 m slip) that ruptured during the earthquake were known to be active prior to the earthquake and incorporated into the National Seismic Hazard Model (NSHM) (Stirling et al., 2012). By contrast, in the NCD, most of the faults were either not known to be active (Leader Fault) or had poorly defined lengths compared to the 2016 ruptures. Therefore, independent of whether these faults generally rupture together or separately, their pre-earthquake fault lengths would produce underestimates of earthquake magnitudes. In addition, the Kaikōura earthquake supports the notion that many active faults in New Zealand remain undetected (or poorly resolved) and have the potential to produce future large-magnitude earthquakes that would not be explicitly accounted for in hazard models (Nicol et al., 2016).

The 2022 New Zealand seismic hazard model contains about 880 individual active faults and permits multi-fault earthquakes generally treats these as discrete sources (Stirling et al., 2012). Large historical earthquakes in New Zealand (Nicol et al., 2022), numerical earthquake simulations (Shaw et al., 2022; Penney et al., 2025) and the latest version of the NSHM (Gerstenberger et al., 2024) all include multi-fault earthquakes, although the Kaikōura earthquake has not been perfectly replicated in the simulations (e.g., Penney et al., 2025). The likely existence of undiscovered active faults and poorly defined multi-fault earthquake scenarios requires that seismic hazard models include large earthquakes (up to at least magnitude 7.8), in the distributed model.

Breaching of the Leader landslide dam could prove hazardous for farming operations, transport networks and people downstream of the dam. Upstream migration of the western knickpoint (see Figure 4) will ultimately lead to breaching of the dam and lowering of Lake Rebekah (assuming no further intervention). Therefore, for risk and lake management purposes, there is value in considering the likely future knickpoint migration rates and associated river incision. Based on knickpoint migration rates since the present river location was established, using data from McCarthy (2025) we estimate that the dam will breach in ~1.5 to ~18 years from January 1 2026 (mean ~3.5 years). This large range reflects uncertainties in bedrock induration and peak river flow rates. When the dam breaches it is most likely to lower Lake Rebekah by 2-4 m and rapidly (within hours to days) release ~300-400 thousand cubic metres of water downstream. The life expectancy of Lake Rebekah following the first dam breach is uncertain, because it is not known whether the river will incise into landslide debris, quaternary deposits or bedrock beneath the present head of the lake. Despite the significant uncertainties, left to natural processes the lake will eventually drain.

Stop Descriptions

Stop 1- Waiau Township

The township of Waiau is approximately 5 km east of the Kaikōura Earthquake epicentre. Due to its proximity to the epicentre and possible peak ground accelerations of up to 3g being recorded near Waiau, 26 buildings in the township were reported to be damaged beyond repair. These heavily damaged buildings were either removed completely or abandoned (Figure 5). All Saints Anglican church is one of the last remaining buildings in the township of Waiau damaged during the earthquake (Figure 5). In the photograph, particularly note the lean on the bell tower, which has detached from the church roof and floor. The church has not been used since the earthquake.

Figure 5. *Photograph of All Saints Anglican Church in Waiau showing earthquake-related damage to the building. Photograph taken in October 2025 by Trevor Willetts.*

Stop 2 - The Humps Fault fence offset

The Kaikōura earthquake originated on The Humps Fault, which is the southwestern-most surface rupture of the Kaikōura earthquake. It strikes east to northeast and extends for ~36 km from a tip on the western margin of the Emu Plains to its junction with the Leader Fault at the base of the Mount Stewart Range in the east (Figure 2). In general, the western section of The

Humps fault (Figure 2) dips steeply to the south, with dips of ~70-90° from surface exposures, aftershocks and the depth of the main shock (~14 ± 2 km) (Nicol et al., 2018). Prior to the Kaikōura earthquake, insufficient information was available to define the length of The Humps Fault or its sense of slip (Barrell and Townsend, 2012). Trenching of The Humps Fault indicates at least six earthquakes on the fault in the last ~15 kyr, with an average recurrence interval of about 3 kyr (Brough et al., 2023).

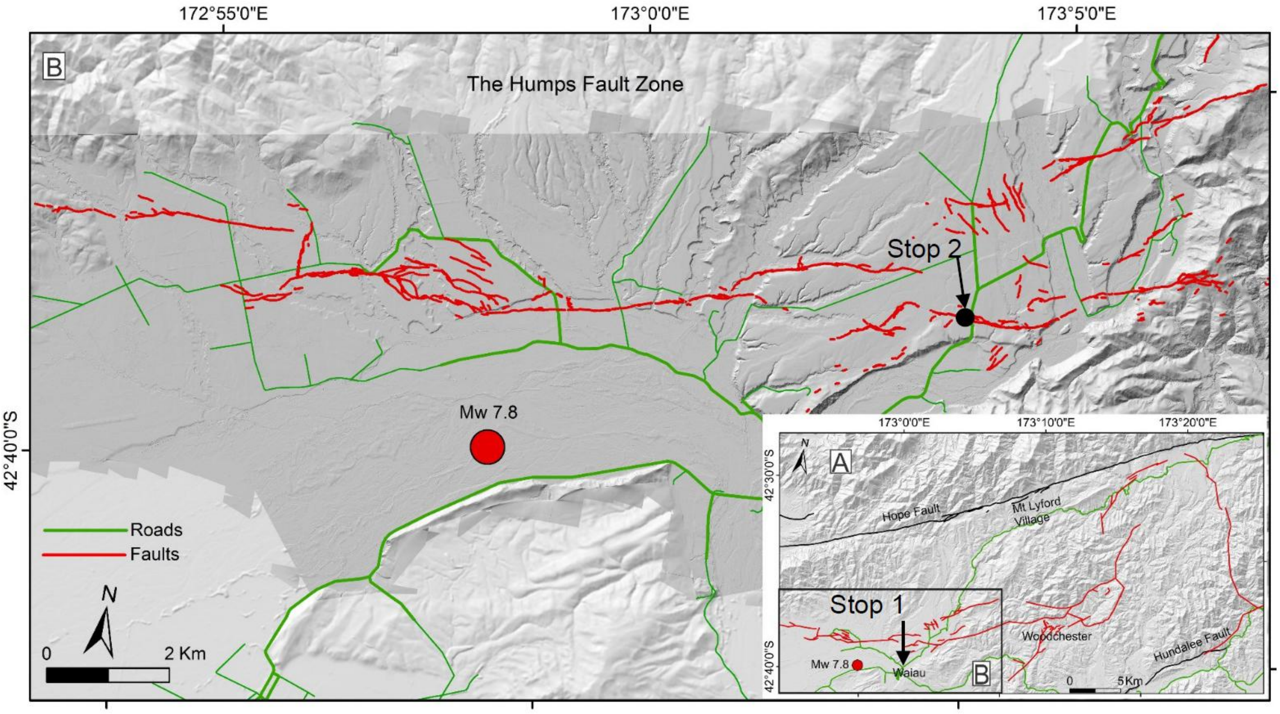

Figure 6. *Overview of the Kaikōura earthquake southern fault ruptures (A) and the Humps Fault Zone (B). The epicentre of the Kaikōura earthquake is shown by the red filled-circle; the rupture initiated on a 80° S dipping dextral reverse fault at ~14 km depth and mainly propagated to the east (Nicol et al., 2018).*

Surface ruptures of the ground surface (e.g. red lines on Figure 6) were primarily mapped using cracks, fissures and displacements of cultural features (e.g., roads, farm tracks, fences and tree lines). The Humps Fault on the Emu Plains is primarily right-lateral. The displaced fence on the Dalmer property provides a good example of the displacements observed along many of the 2016 surface ruptures (see Stop 2 on Figure 2 for location; see Figure 7 for photo of displaced fence). At this locality the fence displays about a metre of right-lateral displacement and approximately half a metre of down throw to the north. Along The Humps Fault right-lateral strike displacement, vertical displacement and net displacement reach values of up to 4 ± 0.3 m, 3.5 ± 0.5 m and 3.9 ± 0.3 m, respectively. Displacement measurements across the alluvial plains display significant variation in both horizontal and vertical displacement. Many of the strike-slip displacement lows are located at steps or branch-points along the fault trace indicating that some of the fluctuations in displacement may reflect fault segmentation. One possible explanation for the coincidence of displacement lows and segment boundaries is that these are sites of elevated off-fault deformation, which is not well sampled by our displacement measurements.

Figure 7. *Photograph (looking north) of displaced fence on The Humps Fault, Dalmer Property, near Waiau (Photograph Kate Pedley).*

Stop 3 Leader Fault and 'Waiau wall'

The Waiau wall fault surface rupture is located on the Leader Fault which has an overall strike of NNE and exhibits primarily left-lateral reverse displacement with throw up to the west (Figures 2, 8 & 9). The fault extends for ~28 km along strike from a tip in the south to its intersection with the Conway-Charwell fault in the north (Figure 2). A complex array of mapped traces ruptured during the earthquake, forming a zone of up to ~3.5 km wide, with strike varying through 180˚, and dips from 80˚ E to 25˚ W (Figure 2 Leader Fault inset stereonet). Along the Leader Fault no active fault scarps were identified prior to the earthquake. Paleoearthquake studies after the earthquake reveal that the Leader Fault probably ruptured at least once in the last 1000 years, although the precise timing of this event remains poorly constrained (Bushell, 2022).

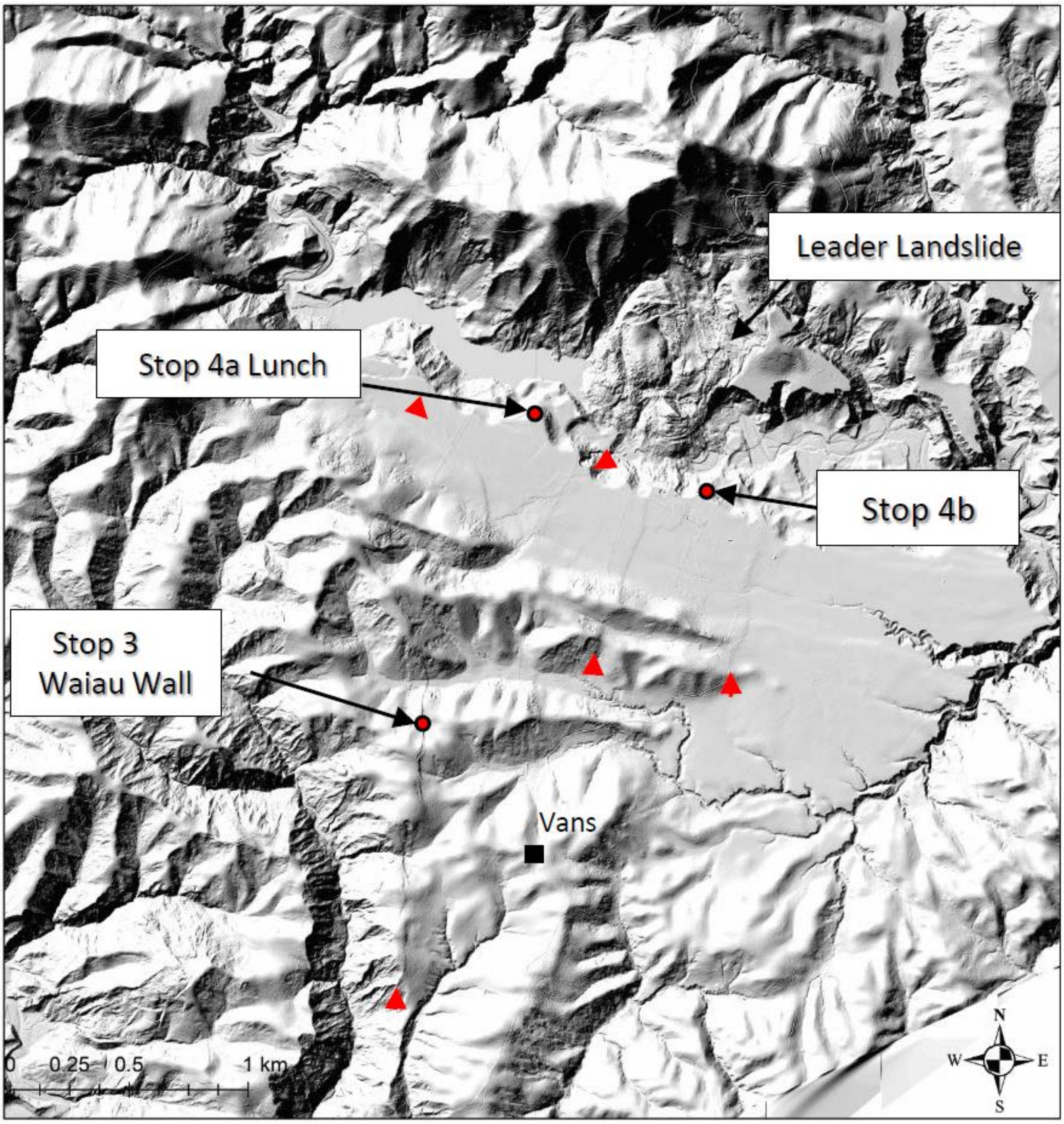

Figure 8. *Hill shaded LiDAR map showing the topography of Woodchester Station and Stops 3 & 4. Red triangles indicate the locations of surface ruptures produced in the 2016 Kaikōura earthquake.*

During the Kaikōura earthquake the Leader Fault primarily accommodated left-lateral reverse displacement, with vertical and horizontal components ranging up to 3.5 m and 3 m (including uncertainties), respectively (Figure 8). The Waiau wall site (Figures 2, 8 & 9) is one locality where the vertical displacement on the fault is significantly above background values. It is possible that some vertical displacement at the Waiau Wall site reflects gravitational rather than tectonic processes, although this hypothesis has not been tested.

When the Waiau wall was freshly exposed it was possible to observe striations on the fault surface (Figure 8D), which are interpreted to record the slip direction of the fault during the earthquake. Interestingly, the orientations of these slickenside striations were more dip slip on the lower two metres of the fault surface. Curvature of the striations down the fault plane suggests that fault slip was initially mostly strike-slip and then a mix of dip slip and strike slip. The reason for the change in slip direction at the Waiau wall locality is presently unclear, although further north on the Kekerengu Fault a similar phenomenon has been observed where it is attributed to the earthquake rupture direction (Kearse et al., 2019). Using this curvature and the model of Kearse et al. (2019), the earthquake may have propagated from north to south along this section of the fault.

Figure 9. *The Waiau wall on Woodchester Station from different perspectives. (A) 26/11/16. Twelve days after the earthquake, with most of the fault forming nearly vertical faces. (B) 6/12/2016. Twenty 24 days after the earthquake. (C) 8/9/2017. Significant ponding along fault scarp; nearly all vertical faces have been degraded; some have soil forming over colluvial wedges. (D) 6/12/2016. Sinistral-oblique slickensides exposed on the scarp; all have now been degraded and cannot be observed. All photographs by Kate Pedley.*

Stop 4 Leader landslide and dam

The primary purpose of this stop is to examine and discuss the Leader landslide and the response of the Leader River to landslide deposition. The Leader landslide was triggered by shaking during the Kaikōura Earthquake. Of the earthquake-induced landslides about 50 collapsed into river valleys and produced large dams that impeded drainage and formed lakes (Figures 3,4 and 10). The Leader landslide dammed the river and took approximately 1 month to form Lake Rebekah. The Leader landslide material mainly comprises weak and low permeability Late Miocene Greta Siltstone Formation. The landslide debris is uncompacted and easily eroded (compared to bedrock and quaternary gravels). The sequence of events for the formation and evolution of the dam is given in Table 1. Most of the key events occurred in the first-year post-earthquake. Unlike many other landslide dams it has not yet fully breached, although without continued human intervention the lake will almost certainly drain in the coming years to decades (see "Implications for hazards" section for further discussion)

***Table 1**. Timeline of key events in the evolution of the Leader River and Lake Rebekah, from the Kaikōura Earthquake (14/11/2016) up to December 2024 (McCarthy, 2025).*

Date/Timeframe (d/m/y)	Event
14/11/2016	Kaikoura earthquake and leader landslide formation
14/11/2016	Lake Rebekah starts to form
Mid 12/2016	Leader dam overtops and western lake forms
Late 01/2017	Middle and east lakes fill
13/02/2017	Partial landslide collapse and drainage adjustments
10/03/2017	Construction of erosion protection bank at western knickpoint
Mid 10/2017	Eastern lake evacuated by eastern knickpoint migration and dam breaching.
2024-onward	Continued migration of western knickpoint

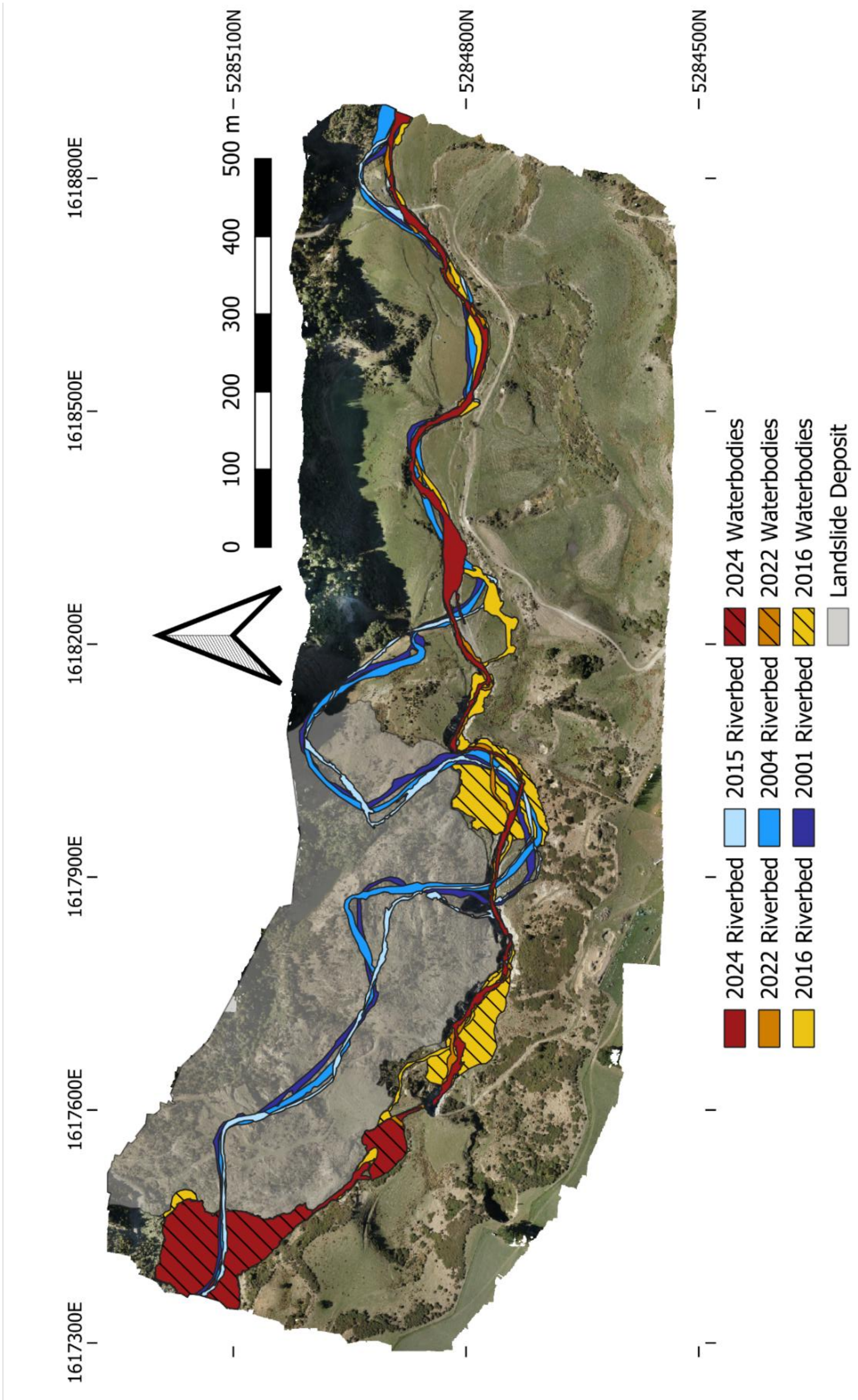

Figure 10. *Map showing the evolution of the Leader River channel prior to and since the 2016 Kaikōura Earthquake. The extent of the Leader landslide is shown in transparent grey, while river positions are shown in blue (pre-earthquake) and red (post-earthquake). Cross hatching shows the locations of water bodies (yellow ephemeral lakes) and red (still present). From McCarthy (2025).*

References

Barnes, P.M., and J.C. Audru (1999). Quaternary faulting in the offshore Flaxbourne and Wairarapa Basins, southern Cook Strait, New Zealand, N.Z. J. Geol. Geophys. 42, 349-367.

Barrell, D.J.A., and D.B. Townsend (2012). General distribution and characteristics of active faults and folds in the Hurunui District, North Canterbury. GNS Science Consultancy Report 2012/113, 45p.

Beanland, S., K. R. Berryman, and G. H. Blick (1989). Geological invesitgations of the 1987 Edgecumbe earthquake, New Zealand, New Zeal. J. Geol. Geophys. 32, 73-91.

Beavan, J., and J. Haines (2001). Contemporary horizontal velocity and strain-rate fields of the Pacific-Australian plate boundary zone through New Zealand. J. Geophys. Res. 106, 741-770.

Beavan R.J., P. Tregoning, M. Bevis, T. Kato, and C. Meertens (2002). Motion and rigidity of the Pacific Plate and implications for plate boundary deformation. J. Geophys. Res. 107(B10), doi:10.1029/2001JB000282.

Beavan, J., M. Motagh, E. J. Fielding, N. Donnely, N., and D. Collett (2012). Fault slip models of the 2010-2011 Canterbury, New Zealand, earthquakes from geodetic data and observations of postseismic ground deformation, New Zeal. J. Geol. Geophys. 55, 207-221.

Bushell, T. (2022). Geometry, kinematics and paleoseismology of The Humps and Leader faults which ruptured during the 2016 Kaikōura earthquake, north Canterbury, New Zealand, Christchurch, New Zealand. PhD Thesis, University of Canterbury.

Cesca, S., Y. Zhang, V. Mouslopoulou, R. Wang, J. Saul, M. Savage, S. Heimann, S.-K. Kufner, O. Oncken, and T. Dahm (2017). Complex rupture process of the Mw 7.8, 201k, Kaikoura earthquake, New Zealand and its aftershock sequence, Earth Planet. Sci. Lett. 478, 110-120.

Clark, K., E. Nissen, J. Howarth, I. Hamling, J. Mountjoy, W. Ries, K. Jones, S. Goldstein, U. Cochran, P. Villamor, S. Hreinsdóttir, N. Litchfield, K. Berryman, and D. Strong (2017). Highly variable coastal deformation in the 2016 MW7.8 Kaikōura earthquake reflects rupture complexity along a transpressional plate boundary. Earth Planet. Sci. Lett. 474, 605 334-344, doi.org/10.1016/j.epsl.2017.06.048.

Dellow, S., C. Massey, S. McColl, D. Townsend and M. Villeneuve (2017). Landslides caused by the 14 November 2016 Kaikoura earthquake, South

Island, New Zealand. Proceedings 20th NZGS Geotechnical Symposium, New Zealand Geotechnical Society: Napier, New Zealand.

Downes, G.L., and D.J. Dowrick (2015). Atlas of isoseismal maps of New Zealand earthquakes, 1843-2003, 2nd Edition. Institute of Geological & Nuclear Sciences monograph 25 (issued as a CD). Lower Hutt: Institute of Geological & Nuclear Sciences.

Eberhart-Phillips D, and S. Bannister (2010). 3-D imaging of Marlborough, New Zealand, subducted plate and strike-slip fault systems, Geophys. J. Int. 182, 73–96, doi:10.1111/j.1365-246X.2010.04621.x.

Eberhart-Phillips, D., M. Reyners, S. Bannister, M. Chadwick and S. Ellis (2010. Establishing a versatile 3-D seismic velocity for New Zealand. Seismological Research Letters, doi:10.1785/gssrl.81.6.992.

Eberhart-Phillips, D., and M. Reyners (2012). Imaging the Hikurangi Plate interface region, with improved local-earthquake tomography, Geophys. J. Int. 190 (2), 1221-1242.

Forsyth, P.J., D.J.A Barrell, and R. Jongens (2008). Geology of the Christchurch Area: Institute of Geological and Nuclear Sciences Geological Map 16: Lower Hutt, New Zealand, GNS Science, 1 sheet + 67 p., scale 1:250,000.

Gray, M. (2018). The Leader co-seismic landslide; characterisation, failure mechanics, and the role of fault rupture. Professional Masters Project, University of Canterbury (Engineering Geology).

Hamling, I., S. Hreinsdóttir, K. Clark, J. Elliott, C. Liang, E.J. Fielding, N. Litchfield, P. Villamor, L. Wallace, T.J. Wright, E. D'Anastasio, S. Bannister, D. Burbridge, P. Denys, P. Gentle, J. Howarth, C. Mueller, N. Palmer, C. Pearson, W. Power, P. Barnes, D. Barrell, R. Van Dissen, R. Langridge, T. Little, A. Nicol, J. Pettinga, J. Rowland and M. Stirling (2017). Complex multi-fault rupture during the 2016 Mw 7.8 Kaikōura earthquake, New Zealand. Science 356, no. 6334, eeam7194, doi: 10.1126/science.aam7194.

Hyland-Brook, N. T. (2018). Geometry and kinematics of the south leader fault: insights from the 2016 MW 7.8 Kaikoura earthquake. MSc Thesis, University of Canterbury.

Kaiser, A., N. Balfour, B. Fry, C. Holden, N. Litchfield, M. Gerstenberger, E. D'Anastasio, N. Horspool, G. McVerry, J. Ristau, S. Bannister, A. Christophersen, K. Clark, W. Power, D. Rhoades, C. Massey, I. Hamling, L. Wallace, J. Mountjoy, Y. Kaneko, R. Benites, C. Van Houtte, S. Dellow, L. Wotherspoon, K. Elwood, and K. Gledhill (2017). The 2016 Kaikōura (New Zealand) Earthquake: Preliminary seismological report, Seismol. Res. Lett. 88 (3), 727-739, doi: 10.1785/0220170018.

Kearse, J., Kaneko, Y., Little, T., Van Dissen, R. J. (2019). Curved slickenlines preserve the direction of rupture propagation. Geology, 47(9), 838–842. https://doi.org/10.1130/G46563.1

Langridge, R.M., Ries, W.F., Litchfield, N.J., ,Villamor, P., Van Dissen, R.J., Barrell, D.J.A., Rattenbury, M.S., Heron, D.W., Haubrock, S., Townsend, D.B., Lee, J.M., Berryman, K.R., Nicol, A., Cox, S.C., Stirling, M. (2016). The New Zealand Active Faults Database. New Zealand Journal of Geology & Geophysics 59, 86-96. DOI: 10.1080/00288306.2015.1112818.

Litchfield N.J., P. Villamor, R. Van Dissen, A. Nicol, P. Barnes, D. Barrell, J. Pettinga, R. Langridge, T. Little, J. Mountjoy, W.F. Ries, J. Rowland, C. Fenton, M.W. Stirling, J. Kearse, U.A. Cochran, K.J. Clark, M. Hemphill-Haley, N. Khajavi, K. Jones, G. Archibald, P. Upton, C. Asher, A. Benson, S.C. Cox, C. Gasston, D. Hale, B. Hall, A.E. Hatem, D.W. Heron, J. Howarth, T.J. Kane, G. Lamarche, S. Lawson, B. Lukovic, S.T. McColl, C. Madugo, J. Manousakis, D. Noble, K. Pedley, K. Sauer, T. Stahl, D.T. Strong, D.B. Townsend, V. Toy, J. Williams, S Woelz, and R. Zinke (in review this issue). Surface Fault Rupture from the Mw 7.8 2016 Kaikōura Earthquake, New Zealand, and Insights into Factors Controlling Multi-Fault Ruptures. Bull. Seismol. Soc. Am. 108(3B): 1496–1520. doi: 10.1785/ 0120170300.

Massey C, Townsend D, Rathje E, Allstadt K, Kaneko Y, Lukovic B, Bradley B, Wartman J, Horspool N, Hamling I, Carey J, Cox S, Davidson J, Dellow S, Holden C, Jibson R, Jones K, Kaiser A, Little M, Lyndsell B, McColl S, Morgenstern R, Petley DN, Rengers F, Rhoades D, Rosser B, Strong D, Singeisen C and Villeneuve M (2018). "Landslides triggered by the Mw 7.8 14 November 2016 Kaikōura earthquake, New Zealand". Bulletin of the Seismological Society of America, 108(3B): 1630-1648. doi: 10.1785/ 0120170305.

Massey, C., D. Townsend, B. Lukovic, R. Morgenstern, K. Jones, B. Rosser and S. de Vilder (2020). "Landslides triggered by the MW 7.8 14 November 2016 Kaikōura earthquake: an update." Landslides 17: 2401-2408.

Mouslopoulou, V., Saltogianni, V., Nicol, A., Oncken, O., Begg, J., Babeyko, A., Cesca, S., Moreno, M. (2019). Breaking a subduction-termination from top to bottom: the large 2016 Kaikōura Earthquake, New Zealand. Earth and Planetary Science Letters 506, 1-10. 506, 1-10.

Nicol, A., B.V. Alloway, and P.J Tonkin (1994). Rates of deformation, uplift and landscape development associated with active folding in the Waipara area of North Canterbury, New Zealand. Tectonics 13, 1321-1344.

Nicol, A., R. Van Dissen, M. Stirling, and M. Gerstenberger (2016). Completeness of the paleoseismic active fault record in New Zealand. Seismological Research Letters 86 (6), 1299-1310. doi:10.1785/0220160088.

Nicol A., N. Khajavi, J. Pettinga , C. Fenton, T. Stahl, S. Bannister, K. Pedley, N. Hyland-Brook, T. Bushell, I. Hamling, J. Ristau, D. Noble and S.T. McColl (2018). "Preliminary geometry, displacement, and kinematics of fault *ruptures in the epicentral region of the 2016 Mw 7.8 Kaikōura, New Zealand, earthquake". Bulletin of the Seismological Society of America, 108(3B): 1521-1539. doi: 10.1785/0120170329.*

Nicol, A., J. Begg, V. Saltogianni, V. Mouslopoulou, O. Oncken and A. Howell (2023). Uplift and fault slip during the 2016 Kaikōura earthquake and late quaternary, Kaikōura Peninsula, New Zealand. New Zealand Journal of Geology and Geophysics 66(2): 263-278.

Nicol, A., N. Khajavi, J. Humphrey, R. Van Dissen, M. Gerstenberger, M. Stirling (2022). Geometries and slip of historical surface-rupturing earthquakes in New Zealand and their application to seismic hazard analysis. Final Report Biennial EQC Grant 16/71. (https://www.eqc.govt.nz/assets/Publications-Resources/Geometries-and-slip-of-historical-surface-rupturing-earthquakes-in-NZ-and-their-application-to-seismic-hazard-analysis.pdf)

Penney, C., A. Howell, T. McLennan, A. Nicol, and B. Fry, 2025. The role of the Hikurangi subduction interface in enabling Kaikōura-like earthquakes: Insights from synthetic earthquake catalogues. Submitted to Seismica December 2025.

Pettinga, J. R., M. D. Yetton, R. J. Van Dissen, and G. Downes (2001). Earthquake source identification and characterisation for the Canterbury Region, South Island, New Zealand, Bull. New Zealand Soc. Earthq. Eng. 34, 282-317.

Rattenbury, M. S., D. B. Townsend, and M. R. Johnston (2006). Geology of the Kaikōura area. Institute of Geological & Nuclear Sciences 1:250 000 geological map 13. 1 sheet + 70 p. Lower Hutt, New Zealand. GNS Science.

Shaw, B.E., B. Fry, A. Nicol, A. Howell, and M.C. Gerstenberger (2022). An earthquake simulator for New Zealand. Bulletin of the Seismological Society of America. doi: 10.1785/0120210087.

Stirling, M. W., G. McVerry, M. Gerstenberger, N. Litchfield, R. Van Dissen, K. Berryman, P. Barnes, L. Wallace, B. Bradley, P. Villamor, R. Langridge, G. Lamarche, S. Nodder, M. Reyners, D. Rhoades, W. Smith, A. Nicol, J. Pettinga, K. Clark, and K. Jacobs (2012). National seismic hazard model for New Zealand: 2010 update, Bull. Seismol. Soc. Am. 102, 1514-1542.

Wallace, L. M., P. Barnes, J. Beavan, R. Van Dissen, N. Litchfield, J. Mountjoy, G. Lamarche, and N. Pondard (2012). The kinematics of a transition from subduction to strike-slip: an example from the central New Zealand plate boundary, J. Geophys. Res. 117, B02405, doi: 10.1029/2011JB008640.

Wang, T., S., Wei, X., Shia, Q. Qiu, L. Lia, D. Peng, R.J. Weldon, S. Barbot (2017). The 2016 Kaikōura earthquake: Simultaneous rupture of the subduction interface and overlying faults, Earth and Planet. Sci. Lett. 482, (2018) 44–51.

Warren, G. (1995). Geology of the Parnassus area. Institute of Geological & Nuclear Sciences 1:50,000 geological map. Lower Hutt, NZ, Institute of Geological and Nuclear Sciences: 1 sheet +36p.

Williams, C.A., D. Eberhart-Phillips, S. Bannister, D.H.N. Barker, S. Henrys, M. Reyners, and R. Sutherland (2013). Revised interface geometry for the Hikurangi Subduction Zone, New Zealand, Seismol. Res. Lett. 84, 1066-1073.

Route Map

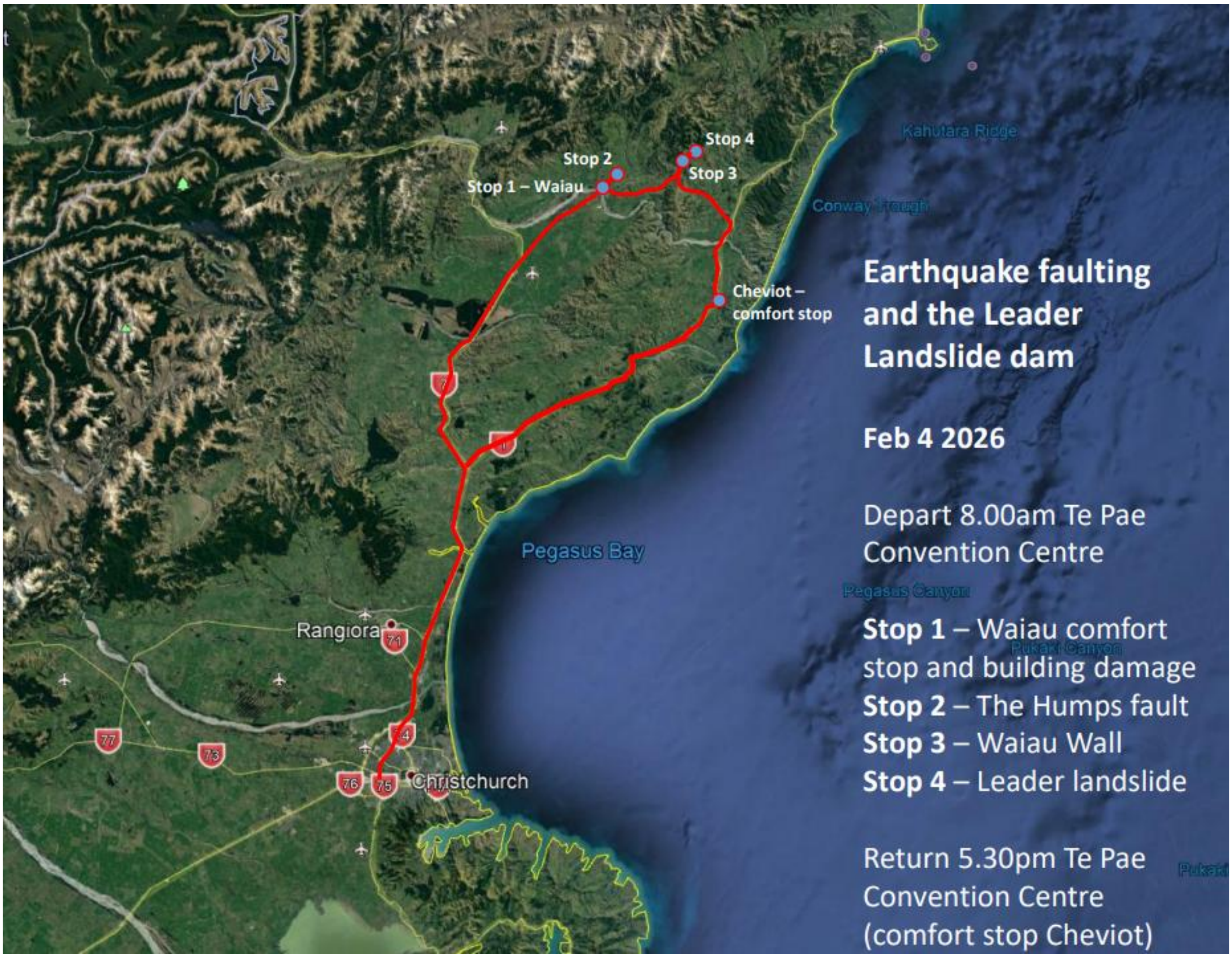

PLATINUM SPONSOR

Earth Sciences New Zealand

GOLD SPONSORS

Environment Canterbury Regional Council
Kaunihera Taiao ki Waitaha

UC University of Canterbury
Te Whare Wānanga o Waitaha
Christchurch New Zealand

SILVER SPONSORS

luminescence dating.
VICUS

Natural Hazards Commission
Toka Tū Ake

BRONZE SPONSOR + YOUNG GEOMORPHOLOGY TRAINING PROGRAM SPONSORS

Zealandia Consulting

EGU European Geosciences Union

BSG British Society for Geomorphology

11TH IAG INTERNATIONAL CONFERENCE ON GEOMORPHOLOGY